# Solvent-Aided Crystallization for Biodiesel Purification

Shafirah Samsuri[1,2]*, Ngiam Li Jian[1], Farah Wahida Jusoh[1], Eduard Hernández Yáñez[3], Nurul Aini Amran[1,2], Noor Yahida Yahya[4]

[1]Chemical Engineering Department, Universiti Teknologi PETRONAS, 32610 Seri Iskandar, Perak, Malaysia

[2]Centre for Biofuel and Biochemical Research (CBBR), Universiti Teknologi PETRONAS, 32610 Seri Iskandar, Perak, Malaysia

[3]Agri-Food Engineering and Biotechnology Department, Technical University of Catalonia-BarcelonaTech, C/ Esteve Terradas, 8, 08860 Castelldefels, Barcelona, Spain

[4]Faculty of Engineering Technology, Universiti Malaysia Pahang, Lebuhraya Tun Razak, 26300 Gambang Kuantan, Pahang, Malaysia

*Correspondence: Shafirah Samsuri (E-mail: shafirah.samsuri@utp.edu.my), Chemical Engineering Department, Universiti Teknologi PETRONAS, 32610 Seri Iskandar, Perak, Malaysia

## Abstract

The application of SAC is based on the addition of solvent (1-butanol) to crude biodiesel to catalyze purification process by separating biodiesel from contaminants via crystallization process. Response surface methodology was applied to optimize the process parameters of SAC, represented by biodiesel purity. The purified biodiesel was analyzed using gas chromatography-mass spectrometry for the composition of fatty acid methyl ester (FAME) present. The predicted optimum process conditions within the experimental ranges for the highest biodiesel purity were 1-butanol concentration of 1.52 wt. %, cooling temperature of 12.7 °C, stirring rate of 175 rpm, and cooling time of 35 min. Under these conditions, the predicted biodiesel purity was 99.375%.
Keywords: 1-butanol, Biodiesel purification, Fatty acid methyl ester, Response surface methodology, Solvent-aided crystallization

## 1    Introduction

Biodiesel is a biodegradable, sustainable, and clean energy, which has attracted worldwide attention as renewable energy and received growing interest in recent years [1]. Biodiesel production in Malaysia is increasing yearly. From 2017 to 2018, total biodiesel that were exported worldwide increased to 332 million liters by 50% and expected to increase by 28% in 2019 [2]. Biodiesel is one of the available renewable energy resources alongside hydropower, wind power, solar power, and others. Biodiesel is the focus of this research because of its application as the fuel source in diesel engines for power generation and biodiesel has cleaner emissions into the environment. The ability of biodiesel to reduce total particulate emissions from engines is an important environmental-benefit property of biodiesel. Autoignition property, which is represented by the fuel's cetane number, is the fuel's ability to auto-ignite. Most biodiesel fuels have higher cetane number than diesel [3].

In Malaysia, few companies such as Malaysian Palm Oil Board, Golden Hope Plantation Sdn Bhd and Emery Oleochemicals applied transesterification reactions for biodiesel production [4]. However, biodiesel produced through transesterification process is unsuitable to be used immediately in diesel engines as impurities are formed during the process, which could damage engines. Crude biodiesel needs to go through purification process to produce highly pure biodiesel, which is measured by the percentage of fatty acid methyl ester (FAME) content and to meet specifications set by the American Society of Testing and Materials (ASTM D6751) and European Norms (EN 14214) [5]. Impurities to be removed include residual quantities of catalyst, glycerol, unreacted alcohol, soap and others.

There are several conventional methods of biodiesel purification such as water washing, acid washing, and washing with ether and adsorbents [6]. Although water washing is efficient, it is associated with the production of waste solutions that would require treatment [7], hence increasing production cost [8]. The water used in biodiesel purification increases the amount of wastewater, thus leading to various environmental effects. Crystallization is widely used as a purification and separation process in industry due to its ability to provide high purity separation. Hence, solvent-aided crystallization (SAC) is suggested as a method to purify biodiesel with the inspiration derived from a case study done by Eisenbart and Ulrich [9]. This separation technique is suitable for high-viscous melts such as glycerol and biodiesel. A solvent is used as an assisting agent to reduce the viscosity of melts. Solvent can affect the nucleation and growth of solid is based on the interaction between the solid surface and the solvent. Solid growth proceed more rapidly as the solvent enters the system. As mentioned by Samsuri et al. [10], crystallization process with addition of solvent will improve separation efficiency. Previous study on biodiesel purification using crystallization without addition of solvent shows that separation efficiency of only 46.734% was achieved [11]. From the study by Eisenbart and Ulrich [9], 1-butanol was used as the solvent to control crystallization kinetics of a water-glycerol mixture.

Therefore, this research attempts to purify biodiesel using SAC method and to obtain the optimum process parameters by applying response surface methodology (RSM) technique and analysis of variance (ANOVA). Furthermore, biodiesel characteristics were determined by analyzing its FAME content using gas chromatography-mass spectrometry (GC-MS) and differential scanning calorimetry (DSC) for thermal analysis.

## 2    Materials and Methods

### 2.1    Materials
The palm oil used for this experiment was the cooking oil from Buruh brand purchased from a local market. Methanol (99.97% purity) and potassium hydroxide (KOH) were supplied by Avantis Laboratory Supply. Ethylene glycol solution of 50% (v/v) with water was used for the coolant. Meanwhile, ethylene glycol and 1-butanol were supplied by Benua Sains Sdn. Bhd.

### 2.2    Methods

#### 2.2.1    Production of Biodiesel via Transesterification Method
Biodiesel was produced using palm cooking oil and methanol as reactants in the presence of KOH as the catalyst. The transesterification reaction was performed in a round-bottom flask equipped with a reflux condenser, a beaker, a magnetic stirrer, a heating and stirring mantle, and a thermometer. 1,000 ml of oil was poured into the flask and heated at 60 °C. Reaction temperature was controlled by the heating mantle. 12.75 g of KOH was dissolved in 225 ml of methanol. The solution of KOH and methanol was then added to the heated oil. The mixture was stirred rapidly for 10 min. The

experimental set-up for transesterification process is shown in Fig. 1. The product obtained is known as crude biodiesel. 1 ml of the product was extracted and put into a glass vial to be tested for its characteristics using gas chromatography-mass spectrometry (GC-MS; Perkin Elmer Clarus 600). The GC was equipped with a flame ionization detector (FID) and Elite 5-MS column (30 m × 250 μm × 0.25 μm film thickness). The initial oven temperature was set at 150 °C, held for 1 min and raised to 240 °C at a ramping rate of 5 °C/min, and then maintained at 240 °C for 5 min. The remaining crude biodiesel was left unattended for 24 h to allow for the separation of biodiesel and glycerol by gravity settling. About 10% of glycerol was produced from transesterification process, as supported by Leoneti et al. [12]. Next, 1 ml of each biodiesel and glycerol was extracted using a syringe and put into a glass vial for DSC analysis to determine its crystallization point. It is important to conduct DSC analysis and determine the crystallization point of biodiesel so that the lowest limit of cooling temperature for SAC process can be determined. In DSC measurement, the biodiesel sample was equilibrated to 30 °C and immediately cooled to -15 °C at a rate of 5 °C/min. Once the sample reached -15 °C, the temperature was maintained for 1 min and then heated to 30 °C at a rate of 5 °C/min. The temperature range for glycerol sample was 0 to 30 °C at the same heating rate (i.e., 5 °C/min).

**Figure 1.** Transesterification system set-up

### 2.2.2   Solvent-aided Crystallization

The experimental set-up for SAC is shown in Fig. 2. The temperature of coolant (ethylene glycol and water) was controlled by a refrigerated bath (630D, PROTECH, Malaysia). The refrigerated bath was turned on and the temperature was set. The temperature range for the whole experiment was between 3.77 and 20.23 °C. Crude biodiesel with glycerol and other contaminants produced from transesterification, as well as 1-butanol, were fed into a cylindrical vessel (13.5 cm × 17 cm). Once the temperature of the coolant had reached the desired temperature, the vessel was placed into the coolant in the refrigerated bath. A stirrer (EURO-ST 40 D S002, IKA, Malaysia) was turned on and the process was left until the end of the desired cooling time. During the process, solid contaminants were formed in layers on the inner cooled surface of the vessel, leaving behind pure biodiesel in liquid form. The goal is to solidify glycerol and contaminants. The purified biodiesel was drained out from the vessel by pouring into a beaker and the solid contaminants were detached from the cooling surface of the vessel and left at room temperature to completely melt. A sample of purified biodiesel was taken for GC-MS analysis to identify for FAME composition which represents biodiesel purity. The experiment was repeated at different values of 1-butanol concentration, coolant temperature, cooling time, and stirring speed. To obtain data at different operating conditions, the entire procedures were repeated from the beginning. The experiment was conducted in accordance to the number of experimental runs required by the design of experiment (DOE) in RSM.

**Figure 2.** Solvent-aided crystallization system set-up

### 2.2.3 Process Optimization

To optimize the process parameters for SAC, RSM was used with the aid of STATISTICA software version 8.0 (Statsoft Inc. USA), which is useful to generate experimental design, full quadratic model, regression analysis, ANOVA, and surface plot analysis. The intended goal is to determine the range of optimum values for each parameter that would yield the desired biodiesel purity.

### (i) Design of Experiment

A five-level-four-factor central composite design (CCD) was employed in this study, requiring 26 experimental runs to construct a second-order response surface model. The parameters involved are 1-butanol concentration (BConc) $X_1$, cooling temperature (CTemp) $X_2$, stirring rate (RPM) $X_3$, and cooling time (CTime) $X_4$, whereas biodiesel purity ($K$) – obtained through GCMS in the form of FAME composition, is the response model from RSM for prediction. The values of low, middle, and high uncoded levels of parameters are listed in Tab. 1.

**Table 1.** Independent variables and levels used for central composite design.

| Parameter | -α | Low | Central | High | +α |
| --- | --- | --- | --- | --- | --- |
| | -2 | -1 | 0 | +1 | +2 |
| BConc, $X_1$ (wt%) | 0.47 | 1 | 1.5 | 2 | 2.53 |
| CTemp, $X_2$ (°C) | 3.77 | 8 | 12 | 16 | 20.23 |
| Stirring Rate, $X_3$ (RPM) | 45.65 | 150 | 200 | 300 | 354.35 |
| CTime $X_4$ (min) | 9.13 | 20 | 40 | 50 | 70.87 |

Using STATISTICA, the parameters studied were input into the software and statistical DOE was generated. The intended response variable was the purity of the purified biodiesel, denoted as $K$. Then, SAC was conducted in repetition for several times using the values of process parameters predicted by the DOE.

The response (i.e., $K$) for each experimental run was tabulated and correlated with the four parameters studied by using multiple regression analysis and employed a second-order polynomial equation generated by the software. The software was also used to analyze the regression, which was then interpreted to determine the significance of each factor investigated. The general form of the second-order polynomial equation is shown by Equation (1) below:

$$Y = \beta_0 + \sum_{j=1}^{4} \beta_j X_j + \sum_{j=1}^{4} \beta_{jj} X_j^2 + \sum_{i<j}^{4} \beta_{ij} X_i X_j \tag{1}$$

Where $Y$ is the response (biodiesel purity); $\beta_0$, $\beta_j$, $\beta_{jj}$, and $\beta_{ij}$ are the intercept, linear, quadratic, and interaction constant coefficients, respectively, that represent the weight of each factor calculated by

STATISTICA to fit the experimental data; and $X_i$ and $X_j$ are the manipulated parameters influencing SAC process.

**(ii) Data Analysis**

One of the criteria to be evaluated for model adequacy is the absolute average deviation (AAD) value, which reveals the summary statistic of statistical dispersion or variability. Therefore, the appropriateness of applying the model to predict SAC optimization can be evaluated. By using the regression model generated, the predicted value for the response in each run of the experimental design was obtained. The adequacy of the generated regression model was evaluated using ANOVA [13]. The $F$-value from ANOVA should be greater than the tabulated value for the model to be considered appropriate [14].

Next, the parameters that would affect the process significantly were identified. A table of multiple regression results was sorted into five columns: factor (parameters), coefficient estimation, standard error, $F$-value, and $p$-value (percentage error). The percentage error was set as 0.05 for 5% error acceptance. This table was used to evaluate the significance of each factor in the model. The factor with the lowest $p$-value (i.e., least percentage error) and the highest $F$-value was considered as the most significant factor. Other factors with a $p$-value higher than 0.05 were determined as insignificant to affect the value of $K$ in SAC.

**(iii) Validation of Optimum Process Conditions**

In this part, SAC process was optimized for obtaining the highest purity of biodiesel. An additional experiment was carried out to validate the optimization results obtained by RSM.

## 3    Results and discussion

### 3.1    Biodiesel Characteristics by Gas Chromatography–Mass Spectrometry

After trial run of the transesterification reaction, the biodiesel was characterized using GC-MS. Fig. 3 shows the chromatograph of biodiesel to study the composition of FAME present. Together with the graph of abundance versus retention time, $t_R$ of biodiesel sample (trial run out of 26 run) and peak data, as shown in Tab. 2, were also obtained to determine the composition percentage and systematic names of methyl esters in the biodiesel sample of trial run.

**Figure 3.** GC-MS chromatograph of biodiesel

Tab. 2 shows the peak data from GC-MS analysis for the biodiesel sample of trial run obtained from gravitational settling. These four highest peaks identified FAMEs as methyl tetradecanoate, hexadecanoic acid, methyl stearate and 9, 12-octadecadienoic acid. From the table, the data such as the correction area of individual components and the sum of correction area were provided and thus, the percentage composition of individual FAME was calculated using Equation (2) in order to determine the biodiesel purity.

**Table 2.** Peak data from GC-MS.

| Peak Number | Retention Time, $t_R$ (min) | Library/ID (Systematic Name) | Trivial Name | Types | Composition of FAME (Purity) % |
|---|---|---|---|---|---|
| 1 | 6.473 | Methyl tetradecanoate | Myristic | Saturated | 1.077 |
| 3 | 9.771 | Hexadecanoic acid | Palmitic | Saturated | 38.287 |
| 5 | 10.122 | 9-Hexadecanoic acid | Palmitoleic | Unsaturated | 0.202 |
| 8 | 13.065 | Methyl stearate | Stearic | Saturated | 4.769 |
| 9 | 13.45 | 9-Octadecenoic acid | Oleic | Unsaturated | 41.876 |
| 11 | 14.143 | 9,12-Octadecadienoic acid | Linoleic | Unsaturated | 11.548 |
| 14 | 15.156 | 9,12,15-Octadecatrienoic | Linolenic | Unsaturated | 0.241 |
| 16 | 16.287 | Eicosanoic acid | Arachidic | Saturated | 0.387 |
| TOTAL | | | | | 98.387% |

$$\%Composition\ of\ FAME = \frac{Peak\ area\ of\ individual\ component}{Sum\ of\ correction\ area} \times 100\% \qquad (2)$$

The calculation for biodiesel purity was then repeated for all significant peaks (% composition not less than 0.1% and methyl esters only). From the calculation for biodiesel purity of trial run, the biodiesel consisted of 98.39% FAME and the components of saturated and unsaturated fatty acids present were 44.52% and 53.87%, respectively. Unrecognized peak found in the chromatograms results in the total FAME content not adding up to 100%. This palm oil biodiesel is composed mainly of methyl esters C16:0, C16:1, and C18:2 which corresponds to methyl palmitate, palmitoleic acid, and linoleic acid respectively. From the composition specifications provided by the Palm Oil Research Institute of Malaysia (PORIM) [15] and crosschecking the specifications with the biodiesel of trial run, it can be concluded that transesterification occurred successfully as the specifications were met. GC-MS was also used to measure FAME yield for all purified biodiesel samples for each SAC run.

## 3.2 Biodiesel Characteristics by Differential Scanning Calorimetry

Fig. 4 presents the graph of heat flow (W/g) against temperature (°C) for the biodiesel sample left unattended to allow gravity settling to occur for 24 h. As observed from DSC analysis (Fig. 4), the biodiesel sample was cooled from 25 to -15 °C, as represented by the blue line. Referring to the vertical line, 9.45 °C indicated the onset temperature that referred to the start of crystallization point of crude biodiesel, which then peaked at 8.4 °C to indicate the highest reaction rate, and later decreased to -5.18 °C, signifying the process ended. Glycerol that has higher crystallization point will solidify as a solid whereas biodiesel that has lower crystallization point will remain in liquid phase [11].

**Figure 4.** DSC curve of biodiesel

## 3.3   Solvent-Aided Crystallization

Crude biodiesel was purified by SAC immediately after the transesterification process. No gravity settling was done before SAC process as the purpose of SAC is to separate and purify biodiesel from glycerol and contaminants. Non-polar solvent such as 1-butanol can influence the solid to be in elongated form [16], as can be seen in Fig. 5 where the glycerol solid formed is in a layer form. It can be observed in Fig. 6 that the denser glycerol (dark-colored liquid) underwent mass transfer, diffused out of biodiesel, and occupied the bottom layer of the liquid system. After subjected to SAC, the purified biodiesel (golden liquid) at the top layer was extracted for GC-MS analysis to determine the FAME composition present. Percentage of FAME composition in the purified biodiesel after the purification by SAC is defined as the biodiesel purity which is calculated using Equation (2).

**Figure 5.** Solid glycerol and liquid biodiesel in the cylindrical vessel

**Figure 6.** Purified biodiesel (gold coloured liquid) and glycerol (dark coloured liquid) after SAC process

## 3.4   Response Surface Methodology

### 3.4.1   Model Adequacy

Multiple regression analysis was carried out using STATISTICA software and a regression equation was generated for $K$ as a function of BConc ($X_1$), CTemp ($X_2$), RPM ($X_3$), and CTime ($X_4$). Their interaction using linear and quadratic regression coefficients of main factors and linear-by-linear regression coefficients of interaction was also derived, as presented in Equation (3):

$$Y = 96.90968 + 1.64831X_1 + 0.00178X_2 + 0.01558X_3 - 0.00896X_4 - 0.29687X_1^2 + 0.00018X_2^2 - 0.00001X_3^2 + 0.00025X_4^2 + 0.00866X_1X_2 - 0.00413\ X_1X_3 - 0.00388X_1X_4 - 0.0002X_2X_3 + 0.00045X_2X_4 - 0.00005X_3X_4 \qquad (3)$$

Where $Y$ is the predicted biodiesel purity. The coefficients with one factor ($X_j$) represent the linear effect of the particular factor, the coefficients with two factors ($X_iX_j$) symbolize the interaction effect between the two factors, and the coefficients with quadratic terms ($X_j^2$) refer to the quadratic effect of the factors. Equation (3) was fitted using the data obtained in Tab. 3.

**Table 3.** Response parameter (K) for each run.

| Run | BConc (X₁) | CTemp (X₂) | RPM (X₃) | CTime (X₄) | K (experimental) | K (predicted) |
|---|---|---|---|---|---|---|
| 1 | 1 | 8 | 150 | 20 | 99.230 | 99.276 |
| 2 | 1 | 8 | 150 | 50 | 98.888 | 99.309 |
| 3 | 1 | 8 | 300 | 20 | 99.626 | 99.629 |
| 4 | 1 | 8 | 300 | 50 | 99.430 | 99.444 |

| 5 | 1 | 16 | 150 | 20 | 99.169 | 99.224 |
|---|---|----|-----|----|--------|--------|
| 6 | 1 | 16 | 150 | 50 | 99.492 | 99.365 |
| 7 | 1 | 16 | 300 | 20 | 99.354 | 99.335 |
| 8 | 1 | 16 | 300 | 50 | 99.309 | 99.258 |
| 9 | 2 | 8 | 150 | 20 | 99.418 | 99.406 |
| 10 | 2 | 8 | 150 | 50 | 99.215 | 99.322 |
| 11 | 2 | 8 | 300 | 20 | 99.007 | 99.139 |
| 12 | 2 | 8 | 300 | 50 | 98.956 | 98.838 |
| 13 | 2 | 16 | 150 | 20 | 99.455 | 99.423 |
| 14 | 2 | 16 | 150 | 50 | 99.616 | 99.448 |
| 15 | 2 | 16 | 300 | 20 | 99.167 | 98.914 |
| 16 | 2 | 16 | 300 | 50 | 98.785 | 98.721 |
| 17 | 1.5 | 12 | 200 | 40 | 99.342 | 99.371 |
| 18 | 0.47 | 12 | 200 | 40 | 99.354 | 99.180 |
| 19 | 2.53 | 12 | 200 | 40 | 98.743 | 98.933 |
| 20 | 1.5 | 3.77 | 200 | 40 | 99.706 | 99.410 |
| 21 | 1.5 | 20.23 | 200 | 40 | 99.044 | 99.356 |
| 22 | 1.5 | 12 | 45.65 | 40 | 99.246 | 99.143 |
| 23 | 1.5 | 12 | 354.35 | 40 | 98.686 | 98.908 |
| 24 | 1.5 | 12 | 200 | 9.13 | 99.532 | 99.577 |
| 25 | 1.5 | 12 | 200 | 70.87 | 99.655 | 99.642 |
| 26 | 1.5 | 12 | 200 | 40 | 99.516 | 99.371 |

Absolute average deviation (AAD) was calculated to verify the model adequacy using Equation (4) [17]:

$$AAD = \frac{1}{n}\sum_{i=1}^{n} \frac{(y_{i,exp} - y_{i,pre})}{y_{i,exp}} \times 100 \qquad (4)$$

Where n is the number of experiments, $y_{pre}$ is the predicted value, and $y_{exp}$ is the experimental value. From the calculation, the AAD value was 0.12%. The model fitted precisely to the experimental data as a low value of AAD between experimental and predicted values was obtained [18, 19]. The more variance that is accounted for by the regression model, the closer the data points will fall to the fitted regression line. Theoretically, if a model could explain 100% of the variance, the fitted values would always equal the observed values.

The F-test compares the model with zero predictor variables (i.e., the intercept-only model) and decides whether the added coefficients improved the model. If a significant result is obtained, then any coefficients included in the model improved the model's fit to the experimental data. From the calculation, the F-value for the model was 1.55 (Tab. 4), which is very close to the minimum of the tabulated F-value of 95% confidence ($F_{0.05, 14, 12}$), which is 2.74. Therefore, the null hypothesis is not rejected.

**Table 4.** ANOVA results for the regression model

| Source | Sum of Squares | Degree of Freedom | Mean Squares | F-value |
|---|---|---|---|---|
| Regression | 1.432583 | 14 | 0.0955 | 1.55 |
| Residual | 0.677726 | 11 | 0.0616 | |
| Total | 2.110309 | 25 | | |
| $R^2$ | 0.67885 | | | |

### 3.4.2    Analysis of Significant Parameters

The interactive term of $X_1X_3$ (BConc and RPM) is the only factor considered by the model to have a significant effect on $K$ with F-value of 6.46 and p-value of 0.027. This is because it is the only factor with p-value less than 0.05 whereas other factors have p-value exceeding 0.05, making other parameters insignificant. This finding is further justified by Fig. 7 that displays the Pareto analysis of the factors.

**Figure 7.** Pareto chart of the interaction of parameters on biodiesel purity

The Pareto chart clearly shows only the bar of the term of interaction between BConc ($X_1$) and RPM ($X_3$) exceeds the right side of the line $p = 0.05$, which implies that this interaction term is a significant factor in SAC. Furthermore, as it is the only term that exceeds the line, the regression model is not entirely rejected, hence justifying the value depicted by the AAD.

### 3.4.3    Response Surface Plot Analysis

Surface plots are useful for investigating the desirable response values and interaction between operating conditions. A circular response surface indicates that the interaction between the corresponding variables is negligible. In contrast, an elliptical or saddle nature of surface plots indicates that the interaction between the corresponding variables is significant [20]. Among the four independent variables studied, three-dimensional (3D) surface was plotted against two independent variables whereas the third and fourth variables were kept constant at the center of their range, as shown in Fig. 8.

**Figure 8.** Response surface contour plots manifesting interactions between factors affecting biodiesel purity

The surface plots of biodiesel purity obtained by Equation (3) at the center point of CCD are displayed in Fig. 8. Fig. 8(a) shows the response surface plot of biodiesel purity for the interaction of parameters between solvent concentration and cooling temperature at the medium value of stirring rate (200 rpm) and cooling time (40 min). From Fig. 8(a), high purity of biodiesel was obtained at low cooling temperature and intermediate concentration of 1-butanol. Non-polar solvent like 1-butanol is suited to oil separation than polar ones. High concentration of 1-butanol reduced biodiesel purity. Although 1-butanol acts as a solvent to increase the solubility of glycerol in biodiesel and also decreases the density difference between glycerol and methyl esters [21], however, too much solvent in a reaction can lead to poor separation. Similarly to the production of highly dry glycerol by Eisenbart et al. [22], small quantities of 1-butanol allowed successful separation of glycerol from water. Hence, the use of an excessive amount of 1-butanol may lead to a state where the viscosity of the solution becomes very high and not favorable for crystallization to take place.

The effect and interaction of solvent concentration and stirring rate are depicted in Fig. 8(b). This surface plot explains that at every value of solvent concentration used, biodiesel purity would increase as the stirring rate increased, up to the intermediate value of both parameters where the purity would peak at 99.5% and then started to decrease to a sharp point at both diagonally opposite ends. The opposite ends of stirring rate that represent low and high speed of stirring caused the low purity. During crystallization, the main impurity which is glycerol formed a solid lattice in the wall surface, leaving the unfrozen biodiesel in the middle of the vessel. Biodiesel molecules are expelled from the solid lattice at the solid-liquid interface and diffuse into the liquid phase. Low stirring rate cannot enhance the movement of crude biodiesel during crystallization as it does not help glycerol to move toward the wall surface. Meanwhile, high stirring rate disrupts the formation of glycerol layer and the layer is mixed with biodiesel. Biodiesel is not easily caught during intermediate stirring rate and is rapidly brought away from the surface of the glycerol solid, causing higher amount of biodiesel remaining in the liquid phase and lower biodiesel entrapment in the glycerol solid. Thus, the efficiency of separation is increased and high purified biodiesel is produced during intermediate stirring rate.

Fig. 8(c) presents the response surface plot of biodiesel purity for the interaction parameters of solvent concentration and cooling time. The high efficiency of the process given by the highest value of biodiesel purity could be observed when solvent concentration is in the range of 0.9 to 2.2 wt. % and not at intermediate cooling time. At this particular cooling temperature (12 °C) and stirring rate (200 rpm), only shorter cooling time is needed for the separation of biodiesel from glycerol and contaminants. This is because glycerol, which is the main contaminant, has high freezing point. Thus, it is easier for glycerol to form solids and separated from biodiesel. When crystallization still occurs, biodiesel tends to be entrapped inside glycerol solids as biodiesel has nowhere to go. However, as more solvent is added, biodiesel purity decreases although at shorter cooling time. These contrasting interactions among the two parameters produced a saddle-shaped response surface, distinctive from previous surface plots.

Fig. 8(d) illustrates the effect of cooling temperature and stirring rate on biodiesel purity. It can be seen from the interaction that intermediate stirring rate gives the best biodiesel purity although cooling temperature changes. In this SAC system, the driving force for nucleation is cooling temperature. Suitable cooling temperature used produces more nuclei during the primary nucleation step of freezing. The rate of primary nucleation depends on cooling temperature [23]. When the suitable temperature reaches, the nucleation is formed, and it could then form an interface between solid and liquid phase. In addition, more nuclei during secondary nucleation can be generated by the

speed of stirring. Once nuclei have formed, the solids grow according to the operating conditions. The stirring causes contacts between growing solids and collisions of solids with the vessel wall, resulting in the formation of new crystal nuclei.

The effect and interaction of cooling temperature and cooling time are shown in Fig. 8(e). The interaction between the two variables can be seen at every point of cooling temperature, which initially produced high biodiesel purity. Increasing cooling time would also decrease biodiesel purity, where the minimum is at the center of response surface, then begins to rise again and peaks are observed at the extreme end. More than 99.9% biodiesel purity can be achieved at high cooling temperature and high cooling time. However, the condition is not preferred as there are more flexible options available, such as the middle region. The influence of cooling temperature on cooling time can be observed at two ends. Firstly, at shorter cooling time, the increase in cooling temperature would reduce biodiesel purity as there is insufficient time for the process to cool for crystallization to occur, hence lower separation efficiency is produced. Secondly, for long cooling time, increasing the cooling temperature would increase biodiesel purity.

Fig. 8(f) shows the response surface plot of biodiesel purity for the combined parameters of stirring rate and cooling time. The interaction of stirring rate and cooling time produces a saddle, hence indicating their influence is indirectly proportional toward each other. The stirring rate starts with high biodiesel purity but drops as cooling time increases, then rises again, and vice versa for the influence of stirring rate on cooling time. This interaction shows that high biodiesel purity was obtained at intermediate stirring rate for a very short or long cooling time. Intermediate stirring rate at specific desired cooling time enhanced the supersaturation distribution rate during crystallization process in the cylindrical vessel by improving crude biodiesel movement near the surface wall. High supersaturation is delayed, which provoked significant growth of glycerol layers after initial nucleation [24]. Solid growth is fast and decrease over time due to increased heat transfer resistance which then lowers the freezing point, making it more difficult to solidify. The decrease of the solid growth rate making less inclusion of biodiesel into the glycerol solid.

### 3.4.4 Optimum Conditions

Upon completing the statistical analysis, STATISTICA generates a set of operating conditions based on the independent variables studied and the model generated (Equation 3). Tab. 5 shows the operating conditions for SAC that the software sets, which predicts the outcome of biodiesel purity of 99.375%. A final experimental run was then conducted using the conditions mentioned to validate the prediction as a form of final reliability test for the model.

**Table 5.** Validation of predicted optimum condition

| Response | $X_1$ (wt%) | $X_2$ (°C) | $X_3$ (RPM) | $X_4$ (min) | Prediction | Validation | Error (%) |
|---|---|---|---|---|---|---|---|
| K | 1.52 | 12.7 | 175 | 35 | 99.375 | 99.49 | 0.12 |

The reliability of the predicted biodiesel purity was checked by calculating the percentage error between the predicted and experimental values. Upon calculation, the obtained error of 0.12% is far below the maximum allowable error between the predicted and validation values of 10%. Therefore, in this case, the model's prediction of biodiesel purity using the stated operating conditions is almost equal to the actual biodiesel purity conducted physically. This also justifies that the regression model can be accepted for predicting biodiesel purity.

## Conclusion

Biodiesel purification using SAC method was evaluated as to its chemical composition. SAC parameters, namely 1-butanol concentration, cooling temperature, stirring rate, and cooling time were studied and optimized. The optimum condition for 99.375% biodiesel purity was achieved at solvent concentration of 1.5 wt. %, cooling temperature of 12.7 °C, stirring rate of 175 rpm, and cooling time of 35 min. The experimental values are in good agreement with the predicted values. The results of p-value test ($p < 0.05$) confirmed the significance of the interactive effect of solvent concentration and stirring rate, with a p-value of 0.0274. As a conclusion, SAC has shown to be effective for biodiesel purification. Soap, glycerol, and methanol were efficiently removed by SAC. SAC generates almost zero wastewater and more environmentally friendly than conventional purification method such as water washing. Studying the SAC process theoretically and experimentally is helpful in improving biodiesel purification.

## Acknowledgment

## Symbols used

| | | |
|---|---|---|
| $F$ | | Measurement of variance of data |
| $K$ | | Biodiesel purity |
| $p$ | | Probability of observing a result |
| $t_R$ | | Retention time in GC-MS |
| $X_1$ | wt % | 1-butanol concentration |
| $X_2$ | °C | Cooling temperature |
| $X_3$ | RPM | Stirring rate |
| $X_4$ | minutes | Cooling time |

## Abbreviations

| | |
|---|---|
| 3D | Three-dimensional |
| AAD | Absolute average deviation |
| ANOVA | Analysis of variance |
| ASTM | American Society of Testing and Materials |
| BFC | Block freeze concentration |
| CCD | Central composite design |
| DOE | Design of experiment |
| DSC | Differential scanning calorimetry |
| EN | European Norms |
| FAME | Fatty acid methyl ester |
| FID | Flame ionization detector |
| GC-MS | Gas chromatography-mass spectrometry |
| KOH | Potassium hydroxide |
| PORIM | Palm Oil Research Institute of Malaysia |
| RSM | Response surface methodology |
| SAC | Solvent-aided crystallization |

## References

[1]      I. M. Atadashi, M. K. Aroua, A. R. Abdul Aziz, N. M. N. Sulaiman, *Renewable and Sustainable Energy Reviews*, **2011***, 15 (9),* 5051-5062. DOI: http://dx.doi.org/10.1016/j.rser.2011.07.051

[2]      A. G. Wahab. GAIN REPORT: Biofuels Annual, Global Agricultural Information Network, Kuala Lumpur, Malaysia, 2018.

[3]      G. Knothe, J. Krahl, J. Gerpen, *The Biodiesel Handbook*, AOCS Press, Champaign, Illinois **2005**.

[4]      W. N. R. Wan Isahak, Z. A. Che Ramli, M. Ismail, J. Mohd Jahim, M. A. Yarmo, *Separation & Purification Reviews*, **2015***, 44 (3),* 250-267. DOI: 10.1080/15422119.2013.851696

[5]      M. Hayyan, F. S. Mjalli, M. A. Hashim, I. M. AlNashef, *Fuel Processing Technology*, **2010***, 91 (1),* 116-120. DOI: https://doi.org/10.1016/j.fuproc.2009.09.002

[6]      D. Y. C. Leung, X. Wu, M. K. H. Leung, *Applied Energy*, **2010***, 87 (4),* 1083-1095. DOI: https://doi.org/10.1016/j.apenergy.2009.10.006

[7]      T. Kubota, M. V. G. de Araújo, D. J. C. de Sá, C. E. Luneli, R. V. Barbosa, L. P. Ramos, S. F. Zawadzki, *Macromolecular Symposia*, **2016***, 367 (1),* 163-167. DOI: 10.1002/masy.201500162

[8]      I. M. Atadashi, *Alexandria Engineering Journal*, **2015***, 54 (4),* 1265-1272. DOI: http://dx.doi.org/10.1016/j.aej.2015.08.005

[9]      F. J. Eisenbart, J. Ulrich, *Chemical Engineering Science*, **2015***, 133,* 24-29. DOI: https://doi.org/10.1016/j.ces.2014.12.060

[10]      S. Samsuri, N. A. N. Rizan, S. H. Hung, N. A. Amran, N. S. Sambudi, *Chemical Engineering & Technology*, **2019**. DOI: 10.1002/ceat.201800505

[11]      S. Samsuri, M. M. Mohd Bakri, *Separation Science and Technology*, **2018***, 53 (3),* 567-572. DOI: 10.1080/01496395.2017.1392975

[12]      A. B. Leoneti, V. Aragão-Leoneti, S. V. W. B. de Oliveira, *Renewable Energy*, **2012***, 45,* 138-145. DOI: https://doi.org/10.1016/j.renene.2012.02.032

[13]      S. Samsuri, N. A. Amran, M. Jusoh, *IOP Conference Series: Materials Science and Engineering*, **2018***, 358,* 012042. DOI: 10.1088/1757-899x/358/1/012042

[14]      M. Jusoh, A. Johari, N. Ngadi, Z. Y. Zakaria, *Advances in Chemical Engineering and Science*, **2013***, Vol.03No.04,* 8. DOI: 10.4236/aces.2013.34036

[15]      W. L. Siew, T. S. Tang, Y. A. Tan, Malaysia, M. Palm Oil Research Institute of, *PORIM : test methods*, Palm Oil Research Institute of Malaysia, Kuala Lumpur **1995**.

[16]      A. T. Karunanithi, C. Acquah, L. E. K. Achenie, S. Sithambaram, S. L. Suib, *Computers & Chemical Engineering*, **2009***, 33 (5),* 1014-1021. DOI: https://doi.org/10.1016/j.compchemeng.2008.11.003

[17]      L. Ma, E. Lv, L. Du, J. Lu, J. Ding, *Energy Conversion and Management*, **2016***, 122,* 411-418. DOI: https://doi.org/10.1016/j.enconman.2016.06.001

[18]      P. Ghorbannezhad, A. Bay, M. Yolmeh, R. Yadollahi, J. Y. Moghadam, *Desalination and Water Treatment*, **2016***, 57 (56),* 26916-26931. DOI: 10.1080/19443994.2016.1170636

[19]      N. B. Ishola, O. O. Adeyemi, A. J. Adesina, V. O. Odude, O. O. Oyetunde, A. A. Okeleye, A. R. Soji-Adekunle, E. Betiku, *Process Safety and Environmental Protection*, **2017***, 111,* 211-220. DOI: https://doi.org/10.1016/j.psep.2017.07.004

[20]    D. Lotfi, M. Anissa, B. Hafsa, B. Djamila, Z. Ihdene, P. y. Bakos, H. Boudjema, *IOSR Journal of Applied Chemistry*, **2015***, 5 (1),* 43-52.

[21]    J. Van Gerpen, G. Knothe, in *Soybeans*, (Eds: L. A. Johnson, P. J. White, R. Galloway), AOCS Press, **2008**, 499-538.

[22]    F. J. Eisenbart, N. Angermeier, J. Ulrich, *Journal of Crystal Growth*, **2017***, 469,* 191-196. DOI: https://doi.org/10.1016/j.jcrysgro.2016.09.001

[23]    P. Nonthanum, A. Tansakul, *Maejo International Journal of Science and Technology*, **2008***, 2 (Special Issue),* 27-37.

[24]    D. Leyland, J. Chivavava, A. E. Lewis, *Separation and Purification Technology*, **2019***, 220,* 33-41. DOI: https://doi.org/10.1016/j.seppur.2019.03.025

## Table captions

**Table 1.** Independent variables and levels used for central composite design

**Table 2.** Peak data from GC-MS

**Table 3.** Response parameter (K) for each run

**Table 4.** ANOVA results for the regression model

**Table 5.** Validation of predicted optimum condition

## Figures with captions
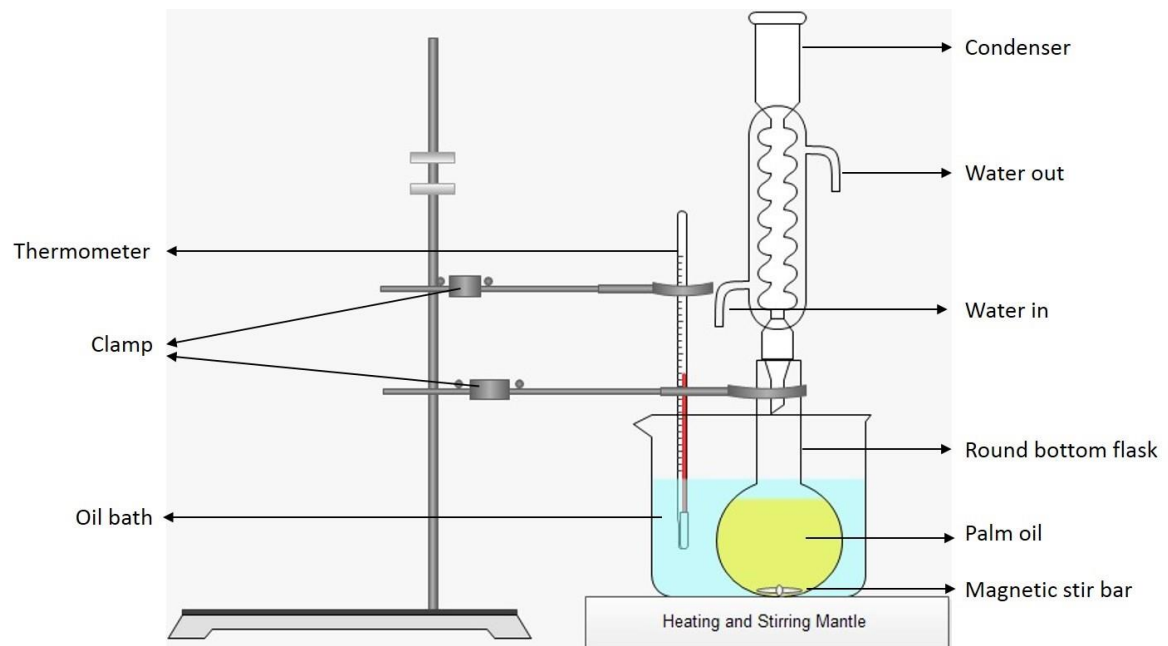


**Figure 1.** Transesterification system set-up
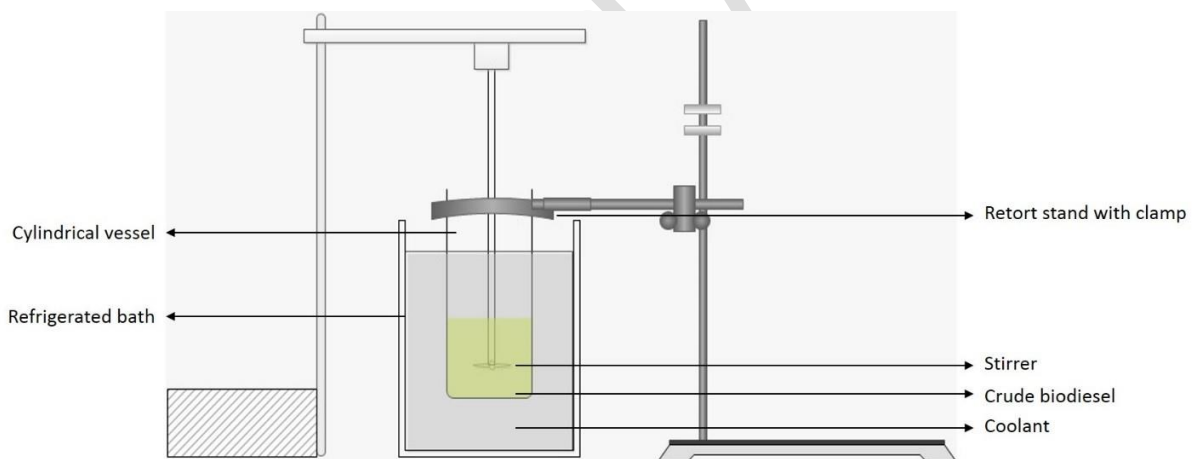
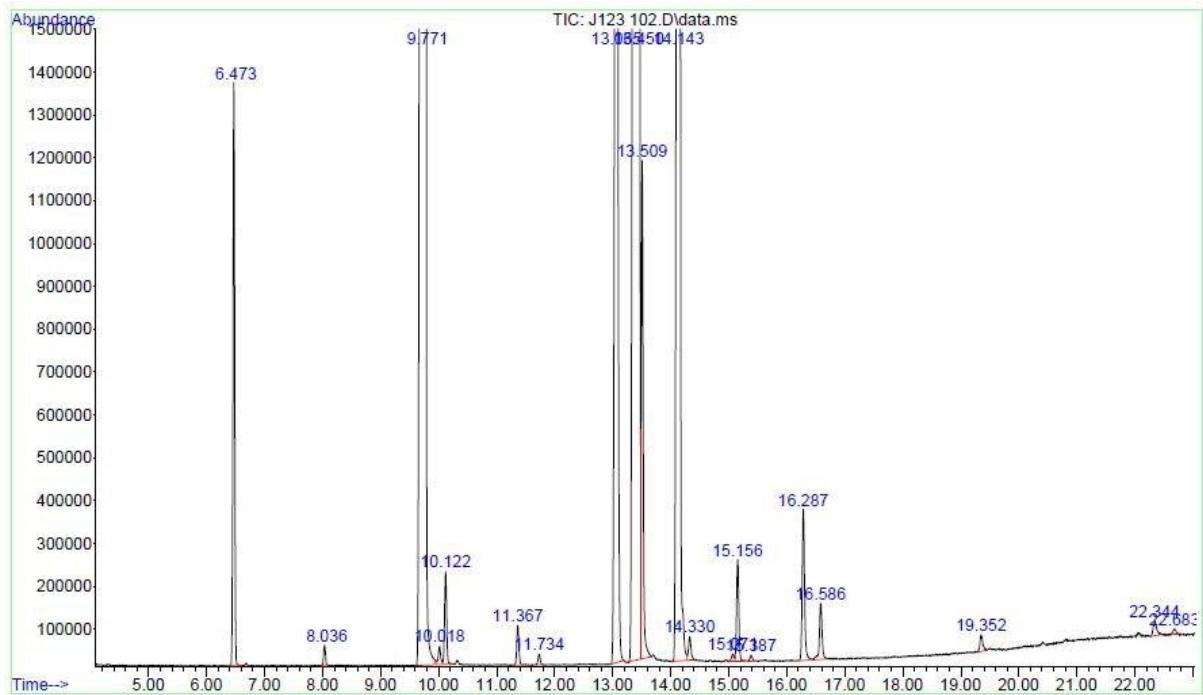

**Figure 2.** Solvent-aided crystallization system set-up
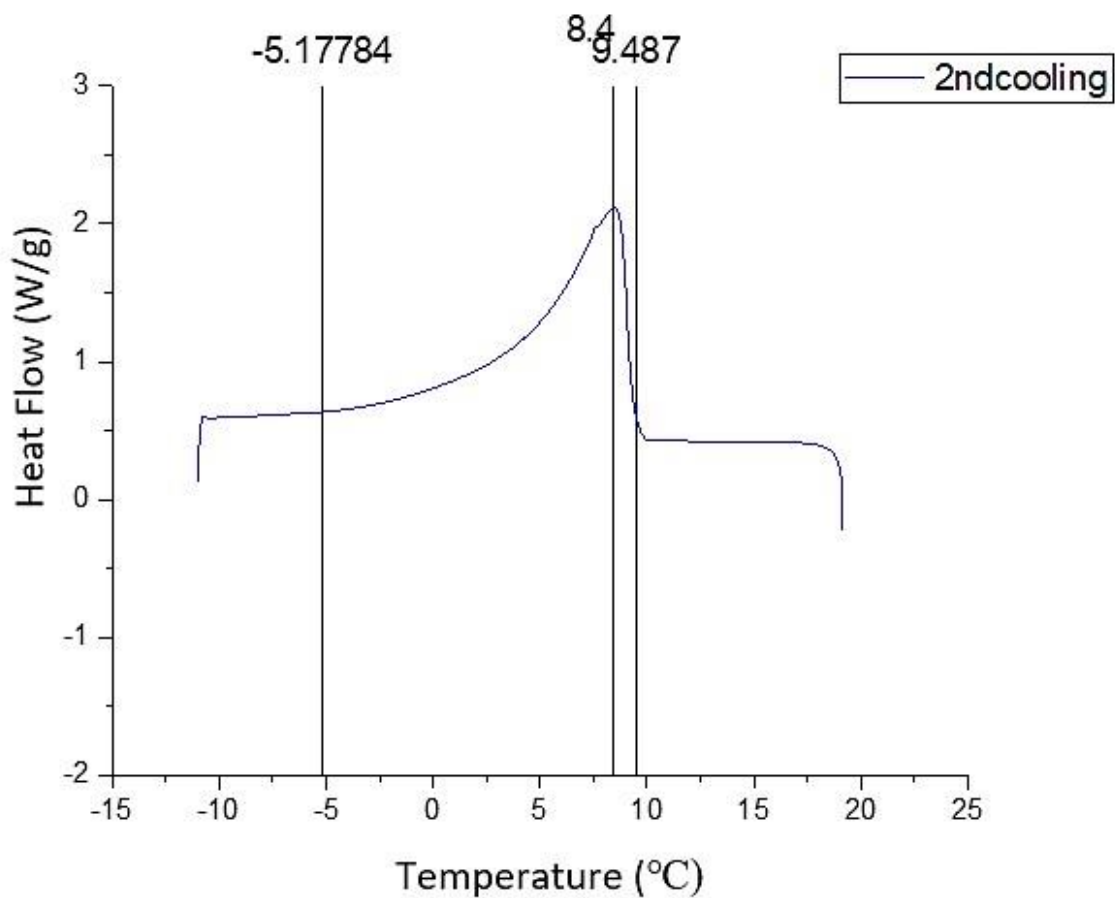
**Figure 3.** GC-MS chromatograph of biodiesel



**Figure 4.** DSC curve of biodiesel

**Figure 5.** Solid glycerol and liquid biodiesel in the cylindrical vessel

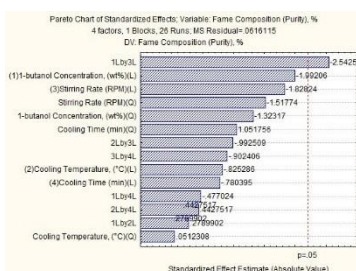**Figure 6.** Purified biodiesel (gold coloured liquid) and glycerol (dark coloured liquid) after SAC process



**Figure 7.** Pareto chart of the interaction of parameters on biodiesel purity
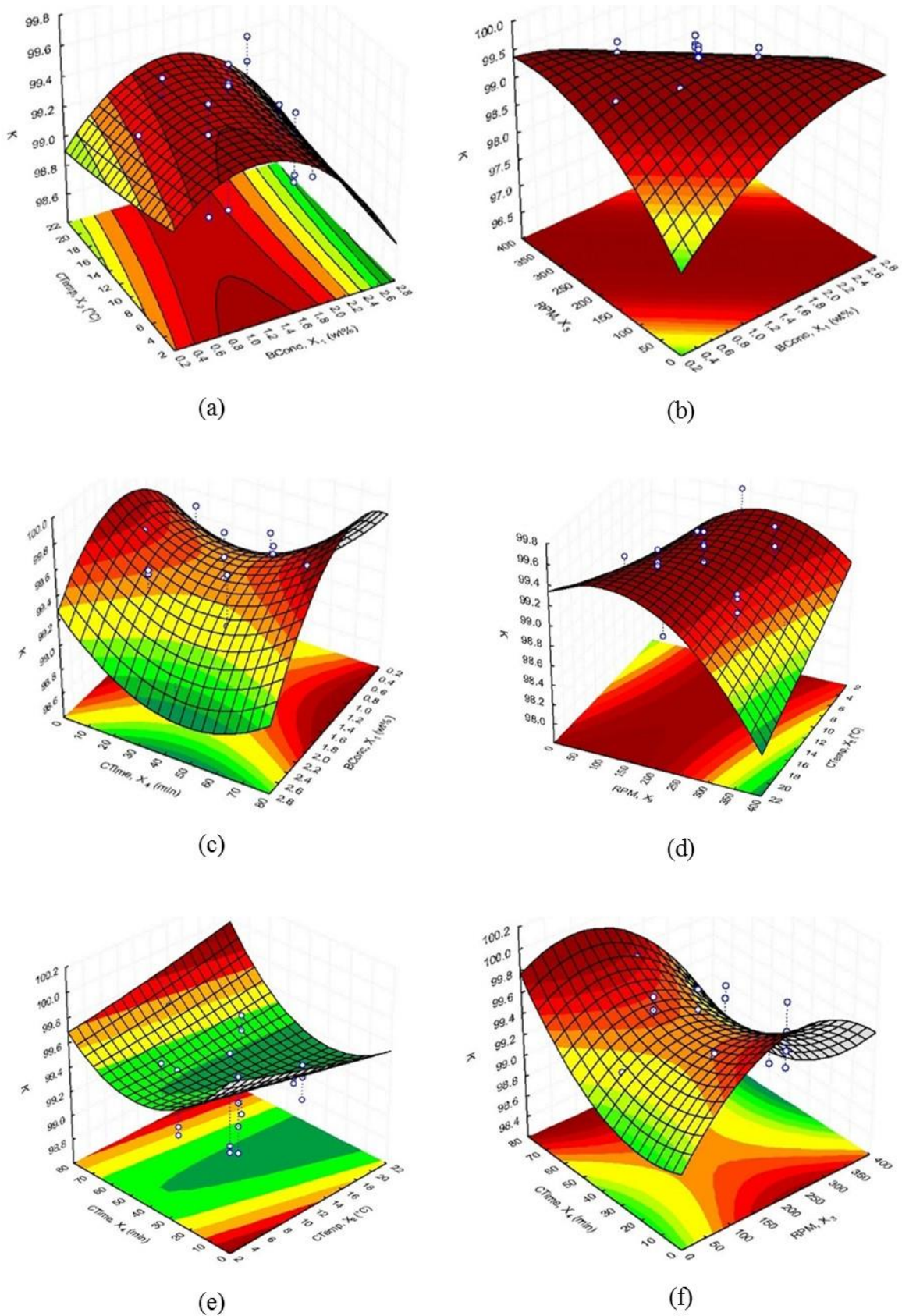
**Figure 8.** Response surface contour plots manifesting interactions between factors affecting biodiesel

purity

## Entry for the Table of Contents

**Type of Article:** Introduction highlights the problem statement and objectives, elaborates the methods for biodiesel purification. Methodology explains the production, purification and analysis of biodiesel. Findings from the performance of biodiesel purification by SAC were discussed in result and discussion.

**Solvent-Aided Crystallization for Biodiesel Purification**
Shafirah Samsuri[1,2]*, Ngiam Li Jian[1], Farah Wahida Jusoh[1], Eduard Hernández Yáñez[3], Nurul Aini Amran[1,2], Noor Yahida Yahya[4]
*Chem. Eng. Technol.* **20XX**, *XX (X)*, **xxxx…xxxx**
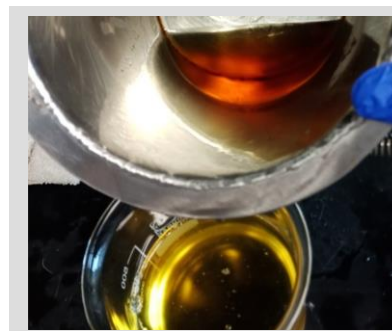


((Pls. indicate if Supporting Information are available))